PO_4 is observed also when all OH^- has been replaced by F^- in synthetic apatites (*4*). Thus one may conclude that carbonate substitutes for phosphate and not for the hydroxyl groups.

The presence of carbonate in synthetic apatites, especially when precipitated at lower temperatures, disturbs the crystallization process (*5*) and increases their solubility (*6*). Carbonate content and susceptibility of teeth to caries have been correlated (*7*). Studies of x-ray diffraction line-broadening and with the electron microscope show that the presence of carbonate causes diminution in size and a change in shape of apatite crystallites. The increased solubility of carbonate-containing apatites thus reflects the increased surface area of the mass of apatite crystallites.

The synthetic apatites studied by us were prepared at 100°C by drop-by-drop addition of 250 ml of $Ca(Ac)_2$ ($0.02M$) solution to 750-ml portions of $0.016M$ Na_2HPO_4 solutions containing also various concentrations (0 to $0.54M$) of sodium carbonate; x-ray diffraction patterns of some of the precipitates appear in Fig. 1. The shift of the 300 and 410 reflections to higher angles demonstrates shortening of the *a*-axis dimensions from 9.43_5 to 9.29_9 Å; shift of the 002 and 004 reflections to lower angles indicates lengthening of the *c*-axis from 6.87_7 to 6.93_2 Å. With increasing carbonate content, the 211 and 112 reflections become superimposed (Fig. 1, D and E).

The breadth of the different peaks varies also (see Fig. 1, A and D or E). In general, increased x-ray diffraction line-broadening results from small crystallite size or from strain in the lattice, or from both. Assuming that the line-broadening in these synthetic apatites is chiefly due to small crystallite size, we determined (from the 002 and 300 reflections) the average crystal dimensions by use of the Debye-Scherer formula (*8*)

$$d_{hkl} = (K\lambda\ 57.3)/(\beta_{\frac{1}{2}} \cos\theta)$$

where the shape-constant K is 0.9, λ is 1.54 Å for $CuK\alpha$ radiation, θ is the diffraction angle, and $\beta\frac{1}{2}$ is line broadening in degrees. The broadening $\beta\frac{1}{2}$ equals the difference between the line breadth (at half-maximum intensity) observed with the samples and that obtained with the very well-crystallized Durango fluorapatite.

In the patterns of carbonate-free apatites we find a greater broadening of the 300 than of the 002 reflections, and therefore conclude that these crystallites must be thin needles elongated along the direction of the *c*-axis. When the apatites richer in carbonate are considered, broadening of the 002 peaks increases more than that of the 300 peaks, an indication that the crystallites have become more "spheroidal," with a length: thickness ratio approaching unity. Electron micrographs of the precipitated apatites confirm these results. Figure 2 shows needle-like crystals for materials very poor in carbonate, and clusters of equiaxed crystals for synthetic materials rich in carbonate.

A possible explanation of the changes in size and shape is that carbonate causes formation of weak bonds, and the growth of a crystal is less in the general direction of the formation of weak bonds than in the general direction of the formation of strong bonds (*9*). The carbonate's interference with the good crystallization of the apatite and its weakening effect on the bonds in the structure increase the rate of dissolution and the solubility. These increases make carbonate-containing dental apatites more susceptible to attack by the weak acids present in the mouth. Thus carbonate contributes to susceptibility to caries.

RACQUEL Z. LEGEROS
OTTO R. TRAUTZ
JOHN P. LEGEROS, EDWARD KLEIN
New York University, 339 East 25 Street, New York 10010
W. PAUL SHIRRA
Philips Electronic Instruments, Mount Vernon, New York

References and Notes

1. W. F. De Jong, *Rec. Trav. Chim.* **45**, 445 (1926).
2. D. McConnell, *J. Dental Res.* **31**, 53 (1962); *Clin. Orthopaed.* **23**, 145 (1962); J. C. Eliott, thesis, Univ. of London (1964).
3. R. Z. LeGeros, *Nature* **206**, 403 (1965).
4. ———, J. P. LeGeros, O. R. Trautz, in *Proc. Intern. Assoc. Dental Res. 43rd Gen. Meeting* (1965).
5. O. R. Trautz and R. Z. LeGeros, *Arch. Oral Biol. Spec. Suppl.* **4**, 122 (1961); J. P. LeGeros, R. Z. LeGeros, O. R. Trautz, in *Proc. Intern. Assoc. Dental Res. 41st Gen. Meeting* (1963).
6. P. Gron, M. Spinelli, O. R. Trautz, F. Brudevold, *Arch. Oral Biol.* **8**, 251 (1963).
7. A. E. Sobel, *Dental Progr.* **2**, 48 (1962).
8. A. Guinier, *X-ray Diffraction in Crystals, Imperfect Crystals and Amorphous Bodies* (Freeman, London, 1963).
9. P. Hartman and W. G. Perdok, *Acta Cryst.* **8**, 49 (1955).
10. We acknowledge support by PHS (grant DE-00159), cooperation by V. Peters (New York Univ.) and R. Markus (Bell Telephone Labs.) in the preliminary electron-micrograph studies, and technical assistance by K. Rajkowski, M. Klein, J. Brand, and C. Strom.

20 November 1966

X-Ray Diffraction Study of Some Fossil and Modern Resins

Abstract. *Samples of both fossil and modern resins have been investigated by x-ray diffraction techniques. Most fossil resins (ambers) yield only diffuse x-ray diffraction patterns, though some (settlingite, Highgate copalite, and guayaquillite) have relatively sharp patterns. Many modern resins, including those from species of* Pinus *and other conifers such as* Picea *and* Abies, *and many of those from* Protium *and* Bursera, *and* Styrax benzoin, *give sharp and distinctive patterns. Some crystalline constituents of the resins which yield the x-ray diffraction patterns have been identified. The similarity between the* Protium *and* Bursera *patterns and those of Highgate copalite and guayaquillite may indicate a possible genetic relationship between these modern and fossil resins.*

Fossil resins, to which the generic term amber usually is applied, have been highly prized and numerous investigations have been made of them. With a view to establishing a genetic relation between fossil and modern resin-producing trees, I have made x-ray diffraction studies of several hundred samples of both fossil resins and resins from modern coniferous and angiosperm trees (*1*). Small samples (approximately 150 mg) of the resins were powdered and spread on a glass slide or pressed into an aluminum holder, in preparation for study in a Norelco x-ray diffractometer. Filtered copper radiation was used.

Most of the fossil resins yielded only diffuse patterns. These patterns are very similar and are characterized by one broad band with its peak between 5.7 Å and 6.2 Å (2θ, 14.3° to 15.55°). Superimposed upon this band and at other positions in the x-ray diffraction spectrum there are minor and, in many cases, sharp peaks that indicate differences in the patterns of the various resins. Figure 1 shows some typical patterns obtained from Baltic Amber (succinite), Austrian copalite, and Mexican Amber from Chiapas. The *d*-spacings for these patterns are given in Table 1. On the basis of these diffuse x-ray patterns alone, it is not yet possible to postulate whether the differences and similarities are due to the botanical origin of the resins or to their various stages of oxidation and polymerization.

The sharp patterns, representing crystalline constituents in the resins, are of particular interest. Only a few of the fossil resins gave such sharp patterns. Among these are copalite from the London Clay at Highgate, settlingite from Settling Stones, England, and guayaquillite from Guayaquil, Ecuador. The constituents responsible for these patterns have not been identified. Both the Highgate copalite and guayaquillite patterns are identical with the resins patterns of modern angiosperm *Protium* and *Bursera*. If the crystalline constituents represented by these patterns have a genetic significance, then possibly the Highgate copalite and guayaquillite have a common origin and may belong to the family of *Burseraceae*, which includes both the genus *Protium* and genus *Bursera*. The patterns for Highgate copalite, guayaquillite, and a *Protium* are shown in Figure 2, and the *d*-spacings are given in Table 1.

The resins of many modern coniferous trees yielded distinctive, and, in some cases, identifiable patterns. Many species of *Pinus* and *Picea* have the same pattern, which, through possibly a mixture of crystalline constituents, appears to contain the naturally occurring crystalline hydrocarbon reficite. Strunz (*2*) has identified reficite with *d*-13^{Δ}-dihydropimaric acid ($C_{20}H_{32}O_2$). The patterns for *Pinus cembra* and *Pinus strobus* are close to that of abietic acid. Frequently, gentle heating induced crystallization of some of the resin components, and, after such treatment, sharper patterns were obtained. In some cases they differed from the patterns of the unheated material. The pattern for *Pinus sylvestris* resin, heated for 2 weeks at 40°C, is much like that of

Table 1. X-ray diffraction data on some patterns of resins. The intensity (*I*) was estimated visually.

Succinite		Copalite (Austria)		Chiapas Amber		Copalite (Highgate)		Guayaquillite		Protium	
d	*I*	*d*	*I*	*d*	*I*	*d*	*I*	*d*	*I*	*d*	*I*
								22.09	3+	22.66	2
						13.00*	< 1	13.2	1	13.4	1
11.63	7									11.63	< 1
						9.66	< 1	9.75	< 1		
								9.41	< 1		
8.60	5					8.67*	1	8.67	3	8.80	2—
						7.69†	2	7.63	6	7.76	3
				7.08	3			7.02	< 1		
				6.56	2						
6.42	4					6.42	10	6.37	10	6.46	10
				6.23	3						
		6.15	10					6.11	4		
6.03	10	6.03	5			5.99	3	5.91	5—	5.99	3
5.76	5	5.83	4	5.85	10	5.80	5	5.76	5	5.83	4
		5.37	4					5.40	3+		
		5.21	3	5.30	4	5.32	6	5.27	5	5.33	5
						5.07*	1+	5.04	3	5.08	2
		4.85	2	4.82	3			4.85	2—	4.72*	4
		4.31	3	4.27	4	4.35†	1	4.37	1+	4.41	2—
										4.19*	< 1
								4.03*	< 1	4.06	< 1
										3.85	< 1
								3.71*	< 1	3.74*	< 1
								3.55	< 1		
				3.36	6	3.33*	2	3.31	< 1		
								3.22*	< 1		

*Broad. †Very broad.

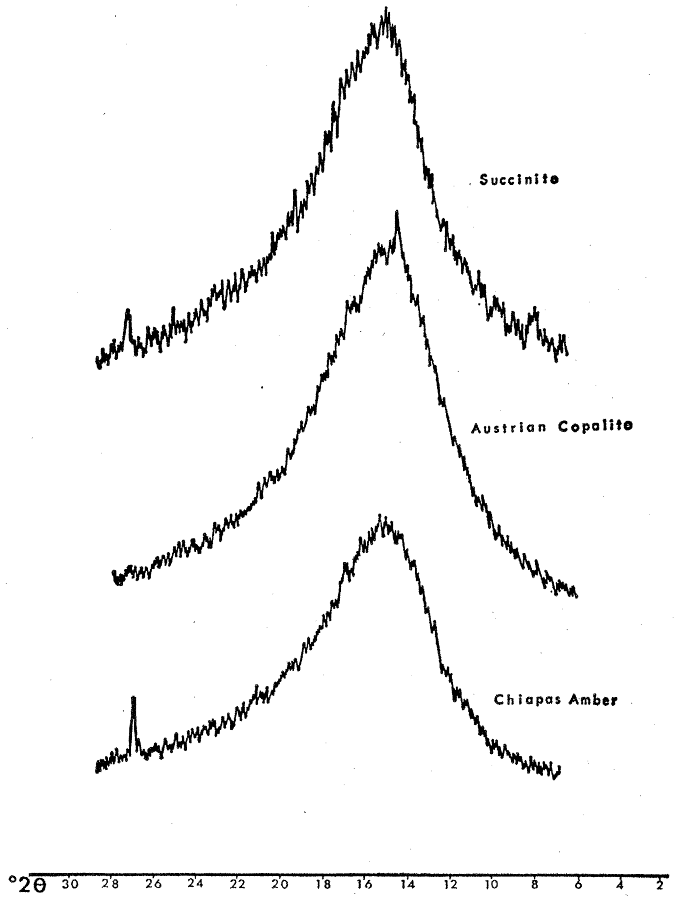

Fig. 1. Diffuse x-ray diffraction patterns of some fossil resins.

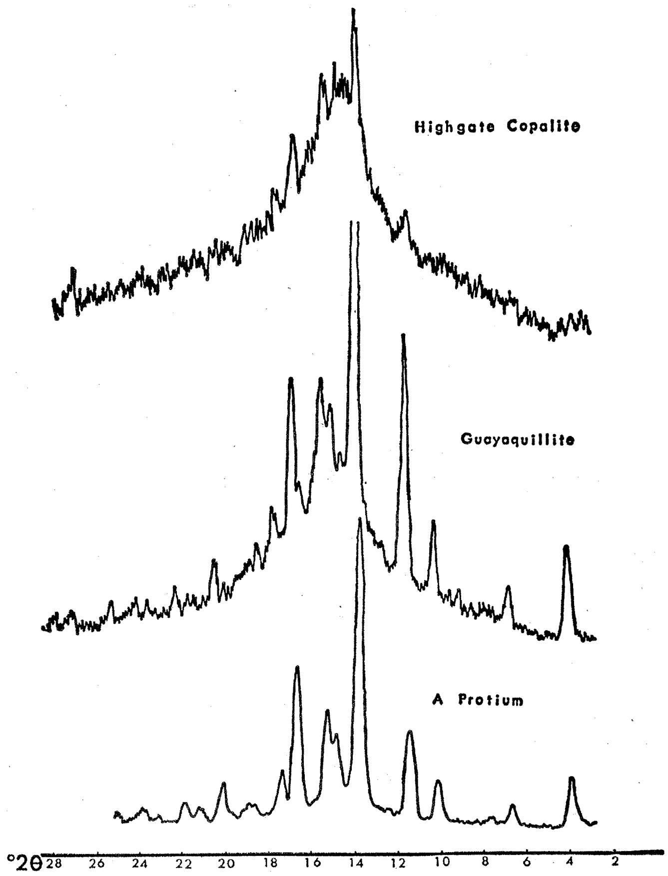

Fig. 2. X-ray diffraction patterns of Highgate copalite, guayaquillite, and a *Protium* resin.

the crystalline hydrocarbon hartite. The pattern of *Abies amabilis* is like that obtained for abietic acid which had been heated 24 hours at 90°C. Resins from some of the *Pinus* species gave distinctly different patterns. These include *Pinus monophylla*, one of the varieties of *Pinus caribaea*, and one of the varieties of *Pinus oocarpa*. Among the resins from angiosperm trees, the pattern for *Styrax benzoin* is essentially that of cinnamic acid.

It may be mentioned here that Pelletier and Walter (*3*) isolated a white crystalline hydrocarbon by dry distillation of succinite (Baltic amber) and that this hydrocarbon was believed to be identical with the naturally occurring hydrocarbon idrialite. Strunz and Contag believe idrialite is identical with picine ($C_{24}H_{14}$). When more such identifications and correlations are made they should aid in revealing genetic relationships between fossil and modern resin-producing trees.

Correlation is needed between results obtained with x-ray diffraction and those of botanists and organic chemists using infra-red absorption spectroscopy and other techniques. It is also necessary to crystallize and identify more individual compounds from these resins for use as standards in the x-ray diffraction study.

JUDITH W. FRONDEL
Hoffman Laboratory, Harvard University, Cambridge, Massachusetts

References and Notes

1. The specimens were obtained from collections of the Harvard University Mineralogical and Botanical Museums, the mineralogical collection of the U.S. National Museum, the mineralogical collection of the British Museum, from Dr. J. Langenheim, and from field collecting at the Arnold Arboretum in Jamaica Plain, Mass.
2. H. Strunz and B. Contag, *Neues Jahrb. Mineral. Monatsh.* **1965-1**, 19 (1965).
3. Pelletier and P. Walter, *J. Prakt. Chem.* **1**, 114 (1844).
4. This investigation was made possible by a scholarship from the Radcliffe Institute, Cambridge, Mass.

20 January 1967

Metastable Superheated Ice in Liquid-Water Inclusions under High Negative Pressure

Abstract. *In some microscopic inclusions (consisting of aqueous liquid and vapor) in minerals, freezing eliminates the vapor phase because of greater volume occupied by the resulting ice. When vapor fails to nucleate again on partial melting, the resulting negative pressure (hydrostatic tension) inside the inclusions permits the existence of ice I crystals under reversible, metastable equilibrium, at temperatures as high as +6.5°C and negative pressures possibly exceeding 1000 bars.*

Liquids can be metastably stretched, under certain conditions, to occupy a larger volume (at a lower density) than that called for at equilibrium. The pressure on the liquid is then less than the (hypothetical) vapor pressure and often less than zero, yielding negative pressures (*1*) that will persist as long as nuclei for a vapor phase are absent. Such negative pressures are of considerable significance in various biological systems (*2*) and are particularly important in boiling or cavitation. I have found no reference to the sustained metastable existence of ice I above its normal melting point of 0°C, such as I have observed in frozen fluid inclusions (*3*). These inclusions yielded possibly the highest negative pressures ever recorded in a static liquid system, although they are still well below the theoretical tensile strength of water (*4*).

Microscopic aqueous fluid inclusions in minerals can be frozen to determine the salinity of the inclusion fluid from its freezing temperature, that is, from the depression of the freezing point (*5*). The equilibrium sequence of phase changes, usually obtained when a frozen inclusion (consisting of saline solution and vapor bubble at room temperature) is warmed, is

$$\begin{aligned} &\mathrm{I + S + V} \rightarrow \mathrm{I + S + L + V} \\ &\quad \sim -50^\circ\mathrm{C} \\ &\rightarrow \mathrm{I + L + V} \xrightarrow{FT} \mathrm{L + V} \\ &\qquad\qquad\qquad < 0^\circ\mathrm{C} \end{aligned} \qquad (1)$$

where I represents ice crystals, S represents salt crystals (mainly $NaCl \cdot 2H_2O$), L is liquid, V is vapor, and *FT* is freezing temperature.

The volume expansion on formation of ice eliminates the vapor bubble in those inclusions, formed at relatively low temperature, which contain only a small vapor bubble (*6*). Inclusions of pure water, in which the vapor is up to 8 percent (by volume) at room temperature, are filled with ice on freezing; the strong brines in some inclusions freeze with only about two-thirds as much expansion (*7*).

When frozen saline inclusions are warmed, there should be a net reduction in volume as the ice and salt mixture melts and dissolves to form ice and brine. (The thermal expansion of the liquid is generally much smaller, as the temperatures are near that of maximum density.) At equilibrium via sequence 1 this volume decrease corresponds to the growth of a bubble consisting of water vapor and gases formerly present as solids such as $CO_2 \cdot 5\frac{3}{4}H_2O$ (*8*). Fluid inclusions are very small systems, exceptionally free from nuclei (*9*); hence they exhibit several metastable phenomena. Once the vapor phase has been eliminated, renucleation is sluggish. Depending upon the quantities of the various phases and the temperatures attained before nucleation, four metastable sequences are possible, and each has been found in natural inclusions:

$$\begin{aligned} &\mathrm{I + S \rightarrow I + S} \overset{M}{+} \mathrm{L} \xrightarrow{R} \mathrm{I + S + L + V} \rightarrow \\ &\qquad \mathrm{I + L + V} \xrightarrow{FT} \mathrm{L + V} \end{aligned} \qquad (2)$$

$$\begin{aligned} &\mathrm{I + S \rightarrow I + S + L \rightarrow I} \overset{M}{+} \mathrm{L} \xrightarrow{R} \\ &\qquad \mathrm{I + L + V} \xrightarrow{FT} \mathrm{L + V} \end{aligned} \qquad (3)$$

$$\mathrm{I + S \rightarrow I + S + L \rightarrow I} \overset{M}{+} \mathrm{L} \xrightarrow{R} \mathrm{L + V} \qquad (4)$$

$$\mathrm{I + S \rightarrow I + S + L \rightarrow I} \overset{M}{+} \mathrm{L} \rightarrow \overset{M}{\mathrm{L}} \xrightarrow{R} \mathrm{L + V} \qquad (5)$$

where *M* indicates a metastable assemblage under negative pressure, and *R* indicates a rapid phase change (*10*).

Sequence 2 is difficult to recognize with certainty, due to the mass of solids present, but the moment of nucleation in 3, 4, and 5 is readily recognized by an apparently instantaneous appearance of a vapor bubble in the liquid and an almost instantaneous melting of ice (Figs. 1 and 2). Because the metastable assemblages may persist for as long as an hour, it is difficult to observe the actual melting of ice when the negative pressure is released. On several occasions, however, other observers and I have witnessed it, and I am certain that there is a definite interval of time (estimated at 0.1 to 0.2 second) over which the melting occurs after nucleation. The melting front must advance through the ice crystal at rates on the order of 200 μ per second.

Sequences 2 and 3 permit valid determinations of the freezing temperature after nucleation of vapor, but 4 and